International Journal of Microwave and Wireless Technologies

cambridge.org/mrf

An ultra-thin polarization independent quad-band microwave absorber-based on compact metamaterial structures for EMI/EMC applications

Naveen Mishra, Khusboo Kumari and Raghvendra Kumar Chaudhary

Department of Electronics Engineering, Indian Institute of Technology (Indian School of Mines), Dhanbad, Jharkhand-826004, India

Research Paper

Cite this article: Mishra N, Kumari K, Chaudhary RK (2018). An ultra-thin polarization independent quad-band microwave absorber-based on compact metamaterial structures for EMI/EMC applications. *International Journal of Microwave and Wireless Technologies* **10**, 422–429. https://doi.org/10.1017/S1759078718000491

Received: 2 September 2017
Revised: 17 February 2018
Accepted: 21 February 2018
First published online: 3 April 2018

Key words:
Absorber; polarization insensitive; ultra-thin

Author for correspondence:
Raghvendra Kumar Chaudhary, E-mail: raghvendra.chaudhary@gmail.com;

Abstract

In this paper, a compact metamaterial inspired ultra-thin polarization independent quad-band microwave absorber for electromagnetic interference (EMI)/ electromagnetic compatibility (EMC) applications have been discussed. The proposed absorber structure offers four different absorption peaks having absorptivity of 97.02, 94.07, 91.72, and 98.20% at 3.40, 8.23, 9.89, and 11.80 GHz, respectively. Due to the four-fold symmetry of the designed unit cell, the proposed absorber structure shows polarization independent behavior. In addition to above, the absorption curve for the designed structure has been also analyzed under different angles of incidence for both transverse electric and transverse magnetic polarization states. In order to confirm the metamaterial behavior of the proposed absorber unit cell, dispersion plot has been studied. Further, input impedance plot, electric field, and surface current distribution plot have been discussed to explain the absorption mechanism of the proposed absorber structure. The designed absorber unit cell shows compactness of $0.136\,\lambda_0 \times 0.136\,\lambda_0$ with the ultra-thin thickness of $0.0113\,\lambda_0$, where λ_0 (free space wavelength) corresponds to the lowest absorption peak of 3.40 GHz. In order to calculate the measured value of absorptivity, the designed absorber structure has been fabricated. Further, it has been observed that simulated and measured results perfectly match with each other. The ultra-thin and compact nature of the proposed absorber structure suggests its potential use in the field of various EMI/EMC applications.

Introduction

Metamaterials [1] are basically artificially engineered electromagnetic media with some exclusive properties that do not occur in nature [1–3]. In the last few years, metamaterials have been used in the field of research for several microwave devices such as antenna [4, 5], filter [6], cloaking [7], super-lens, [8] and absorber [9–11]. In 2008, Landy et.al proposed first "Perfect Metamaterial Absorber" [12]. Since then, metamaterials play a crucial role for absorber applications related to microwave [13], terahertz (THz) [14], infrared, [15] and optical frequency regime [16]. The various advantages of metamaterial absorber include compactness, ultra-thin thickness, near unity absorption and ease of fabrication. A metamaterial absorber basically composed of resonators, arranged periodically on the surface of the dielectric substrate. In order to completely restrict the transmission of electromagnetic waves, the back portion of the substrate is full metal laminated. Hence, to achieve near unity absorption, reflections from the surface of the absorber structure must be reduced. For this purpose, the input impedance of the absorber structure must be nearly equal to free space impedance of 377+j0 ohm. In the previous years, several absorber structures have been reported in single band [17], dual band [18, 19], triple band, [20–22] and multiband [23–26] applications. In [23], the unit cell has four scaled version of flower-shaped structure, which is responsible for the origination of four bands. But due to this arrangement, the unit cell size of the absorber structure has been increased. Article [26] is dealt with a multilayer metamaterial structure to create multi-band polarization-insensitive response. Due to multilayer configuration, the thickness of the proposed absorber structure increases, hence become unsuitable for ultra-thin applications. In order to resolve the issue of large unit cell size and high thickness, the proposed absorber unit cell has been configured with two resonators.

In this paper, a compact metamaterial inspired ultra-thin polarization independent quad-band microwave absorber for electromagnetic interference (EMI)/ electromagnetic compatibility (EMC) applications have been presented. The proposed absorber offers four absorption peaks of 97.02, 94.07, 91.72, and 98.20% at 3.40, 8.23, 9.89, and 11.80 GHz, respectively. Further, the proposed absorber structure has been studied at different polarization angles and oblique incidence angles under both transverse electric (TE) and transverse magnetic (TM) polarization states. The absorption mechanism for the proposed structure has been

CAMBRIDGE UNIVERSITY PRESS

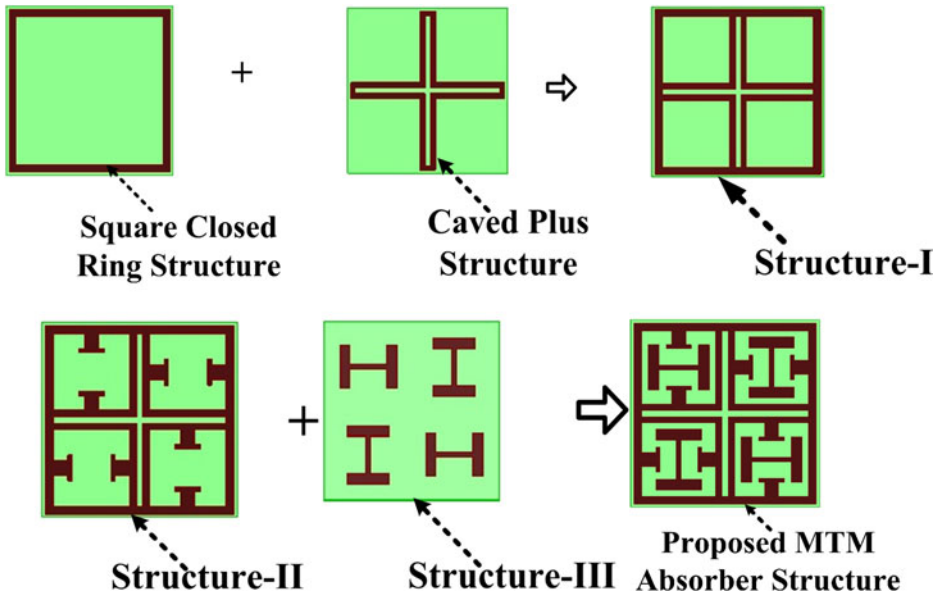

Fig. 1. Different developing stage of the proposed MTM absorber structure.

explained through electric field distribution, current density, and input impedance plots. Since the electrical size of metamaterial (MTM) is very small, hence this can offer an advantage in the construction of several EMC/EMI components.

Design and simulation results

Figure 1 signifies the different developing stage of the designed MTM absorber structure while the geometrical configuration of the top view of the proposed absorber unit cell along with direction of wave propagation, electric and magnetic field vectors has been shown in Fig. 2. The top layer of the designed absorber structure is the combination of structure-II (structure-II is the modified version of structure-I) and structure-III, printed on two-sided copper coated 1 mm FR-4 epoxy dielectric substrate (ε_r = 4.4, tanδ = 0.02). The bottom layer of the designed absorber is completely laminated with 0.035 mm thick copper sheet. The optimized geometrical dimension has been shown in Fig. 2.

ANSYS HFSS 3-D simulation software with master and slave periodic boundary condition and floquet port excitation has been used to analyze the absorptivity of the designed absorber unit cell. The mathematical expression for calculating the absorption coefficient of the designed absorber structure has been represented by Equation (1) as,

$$A = 1 - |S_{11}|^2 - |S_{21}|^2. \quad (1)$$

Since the full copper laminated bottom layer of the designed absorber prohibits the transmission of incident electromagnetic waves, the transmission coefficient is zero and Equation (1) is reduced to Equation (2) as,

$$A = 1 - |S_{11}|^2, \quad (2)$$

where $|S_{11}|^2$ represents reflected power and $|S_{21}|^2$ represents transmitted power. In order to achieve near unity absorption, reflected power $|S_{11}|^2$ should be reduced to zero, as revealed from Equation (2).

The absorption curve for different developing stages of the structure-I has been discussed in Fig. 3.The absorption curve

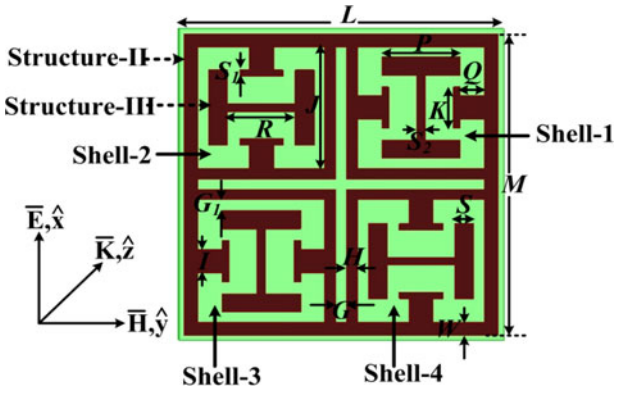

Fig. 2. Top view of the designed metamaterial absorber unit cell with optimized geometrical dimensions (unit: mm): L = 12, M = 11.6, P = 2.9, R = 2.5, Q = 0.9, S = 0.7, S_1 = 0.25, S_2 = 0.3, I = 0.9, J = 4.7, K = 1.6, G = 0.4, G_1 = 0.4, H = 0.4, W = 0.5.

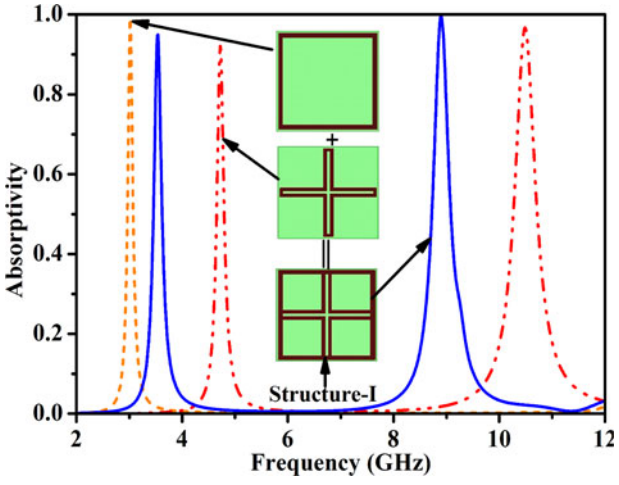

Fig. 3. Simulated absorption curves for different stages of structure-I.

for square closed ring exhibits absorption peak of 99.07% at 3.02 GHz, while caved-plus shaped structure offers two absorption bands with peak absorption value of 92.10% at 4.72 GHz

https://doi.org/10.1017/S1759078718000491 Published online by Cambridge University Press

and 96.73% at 10.49 GHz. The combination of above two structures (structure-I), results in two absorption bands with peak absorptivity of 94.95 and 99.67% at 3.54 and 8.90 GHz, respectively. Further, structure-II which is the modification in structure-I, shown in Fig. 4, is responsible for the origin of a new absorption peak at 11.58 GHz with peak absorption value of 84.41%. On the other hand, the absorption curve for Structure-III (combination of four 90° rotated H-shaped structures) exhibits one absorption peak of 94.37% at 10.43 GHz.

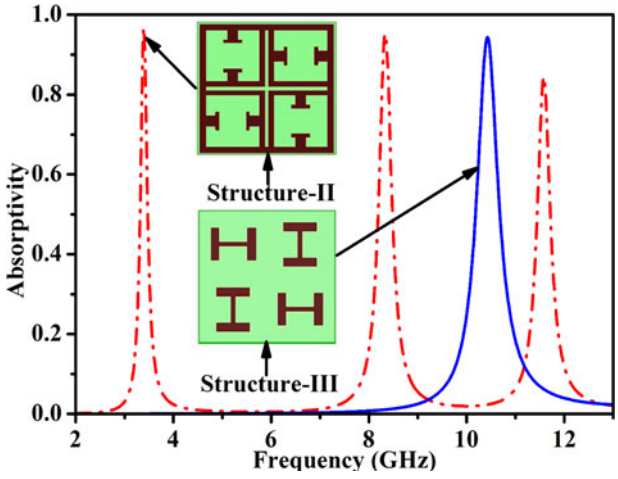

Fig. 4. Simulated absorption curves for structure-II and structure-III.

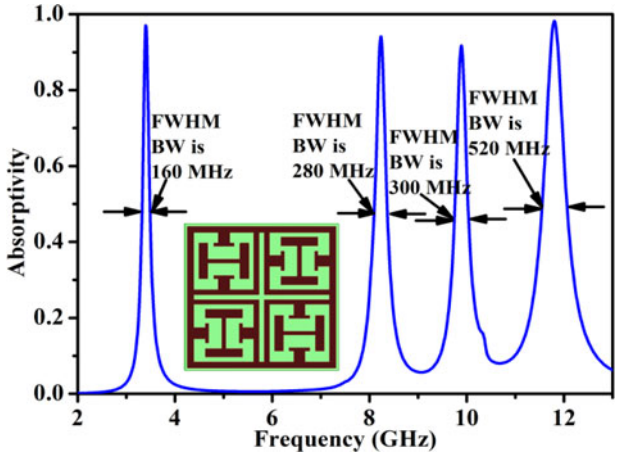

Fig. 5. Simulated absorption curve for the designed absorber unit-cell.

When structure-III is embedded inside structure-II, the designed unit cell corresponds four distinct absorption bands with peak absorption value of 97.02, 94.07, 91.72, and 98.20% at 3.40, 8.23, 9.89, and 11.80 GHz respectively, as shown in Fig. 5. The FWHM (full width at half maximum) Bandwidths of designed quad-band absorber are 160 MHz (3.32–3.48 GHz), 280 MHz (8.09–8.37 GHz), 300 MHz (9.74–10.04 GHz), and 520 MHz (11.54–12.06 GHz).

In order to confirm the polarization independent behavior, designed unit cell has been studied at distinct angles of polarization (0° to 90° in step of 15°), shown in Fig. 6. It has been observed that the value of all four absorption peaks remains the same with the increase of polarization angles. Hence, the absorber is polarization independent.

The designed structure has been also investigated under distinct angles of oblique incidence (0° to 90° in step of 15°) for TE and TM polarization, shown in Figs. 7(a) and 7(b), respectively. For both the polarization state, a high absorption (greater than 80%) has been achieved up to 30° of incidence angle. The increment in incidence angle corresponds to a decrement in absorption peak and this is due to a reduction in incident magnetic flux between the top and bottom surfaces of the designed absorber structure. The variation in incidence angle is responsible for the origin of two more small absorption peaks at 8.23 and 9.89 GHz.

The metamaterial nature of designed absorber unit cell has been illustrated through dispersion diagram plot which is calculated by Equation (3) [27] and shown in Fig. 8. Dispersion diagram plot contains left-handed (LH) and right-handed (RH) region. In case of LH region ($\beta < 0$), the direction of phase and group velocity are aligned opposite to each other, constituting a backward wave but for RH region ($\beta > 0$), phase and group velocity are aligned in the same direction, resulting in a forward wave. It has been observed that the entire FWHM bandwidth of first, second and fourth absorption band lies in LH region while a part of third absorption band lies in LH region, which confirms metamaterial nature of designed absorber structure.

$$\beta d = \cos^{-1}\left(\frac{1 - S_{11}S_{22} + S_{12}S_{21}}{2S_{21}}\right). \tag{3}$$

The electric field distribution and current density plots have been discussed to analyze absorption behavior of the designed

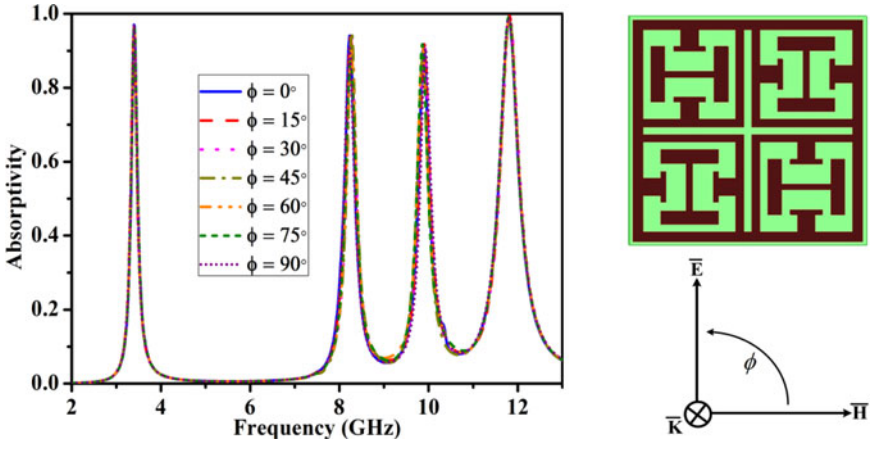

Fig. 6. Simulated absorption curve for the designed absorber structure at distinct angles of polarization. (a) TE polarization, (b) TM polarization.

https://doi.org/10.1017/S1759078718000491 Published online by Cambridge University Press

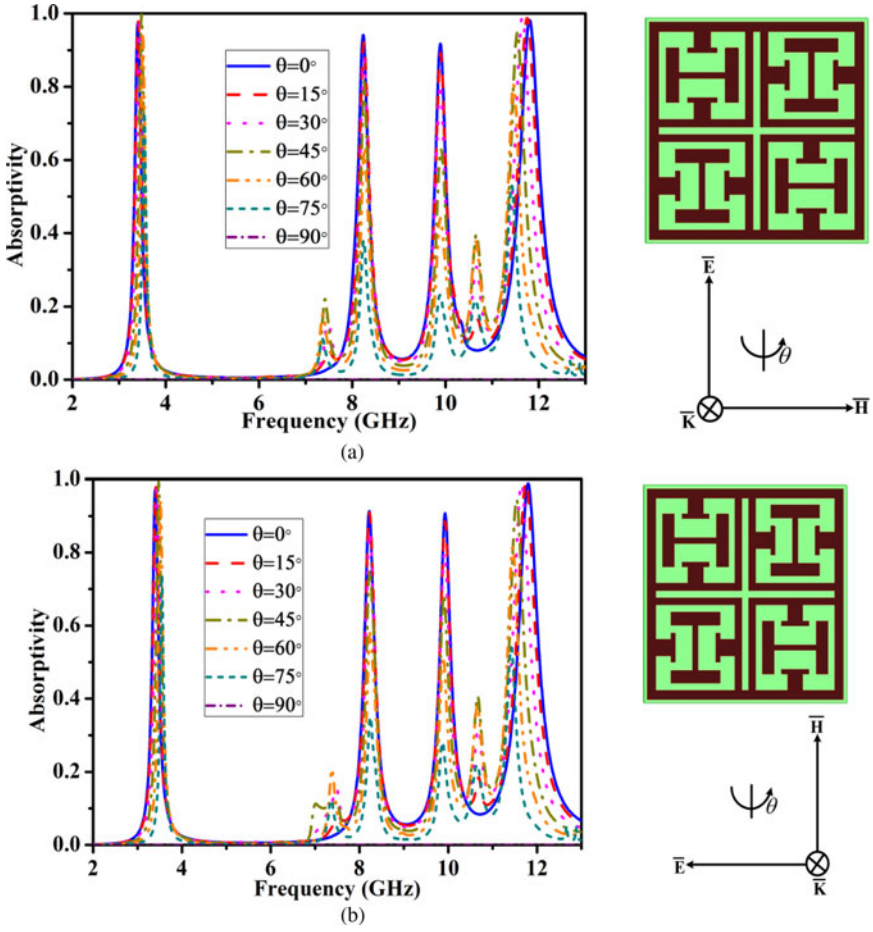

Fig. 7. Simulated absorption curve for the designed absorber structure at distinct incident angles.

absorber structure. Figure 9 shows electric field distribution plot for the designed absorber structure at all the absorption frequencies. It is observed that outer square closed ring is responsible for the origination of lower absorption peak at 3.40 GHz while absorption peak at 8.23 GHz is achieved mainly due to caved-plus patch. At 9.89 GHz, the absorption peak is produced due to the effect of thin rectangular copper strip attached to small square patch in shell 1 and shell 3 and caved-plus patch. Structure-II is responsible for the occurrence of the absorption peak at 11.80 GHz and the coupling between structure-II and structure-III improves the absorption at 11.80 GHz. Hence, an electric excitation has been developed in the top metallic patch at all the absorption frequencies.

Current density plot at all the absorption frequencies on top and bottom surfaces of designed absorber unit cell has been shown in Fig. 10. At 3.40 GHz, the current density is mainly localized in a caved-plus patch along with outer square closed ring resonator while most of the current is mainly distributed on the edges of the caved-plus patch at 8.23 GHz. A high density of surface current at 9.89 GHz flows on the H-shaped patch placed inside shell-2 and shell-4 of structure-II, whereas at 11.80 GHz, the current density is concentrated on outer square closed ring resonator along with H-shaped structure embedded inside shell-2 and shell-4 of structure-II. It is also seen that the direction of flow of surface current at all frequencies on top and bottom surface are anti-parallel to each other, thus creates a circulating current loop, responsible for magnetic excitation. This electric and magnetic excitation is responsible for strong absorption of EM wave.

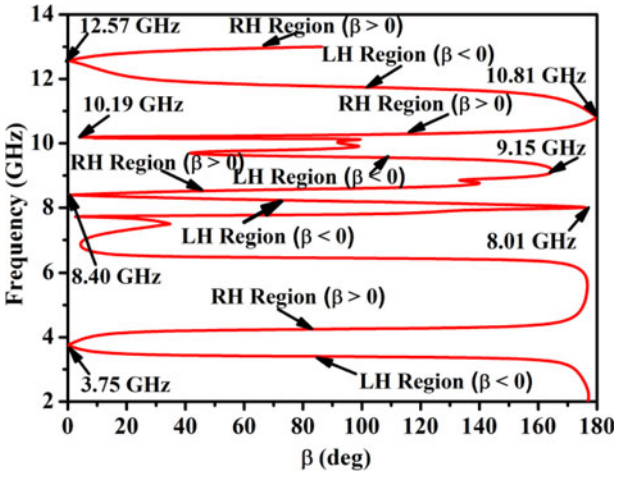

Fig. 8. Dispersion diagram plot for the designed absorber structure. (a) At 3.40 GHz, (b) at 8.23 GHz, (c) at 9.89 GHz, (d) at 11.80 GHz.

In addition to this, input impedance plot has been also studied to explain the absorption behavior of designed absorber structure. It has been observed from Fig. 11 that the value of input impedance at 11.80 GHz ($426.3 \pm 0.955j$) is closely matched to free space impedance ($377 + 0j$), hence a high absorption of 98.20% has been achieved. Further, input impedance at 3.40 GHz

https://doi.org/10.1017/S1759078718000491 Published online by Cambridge University Press

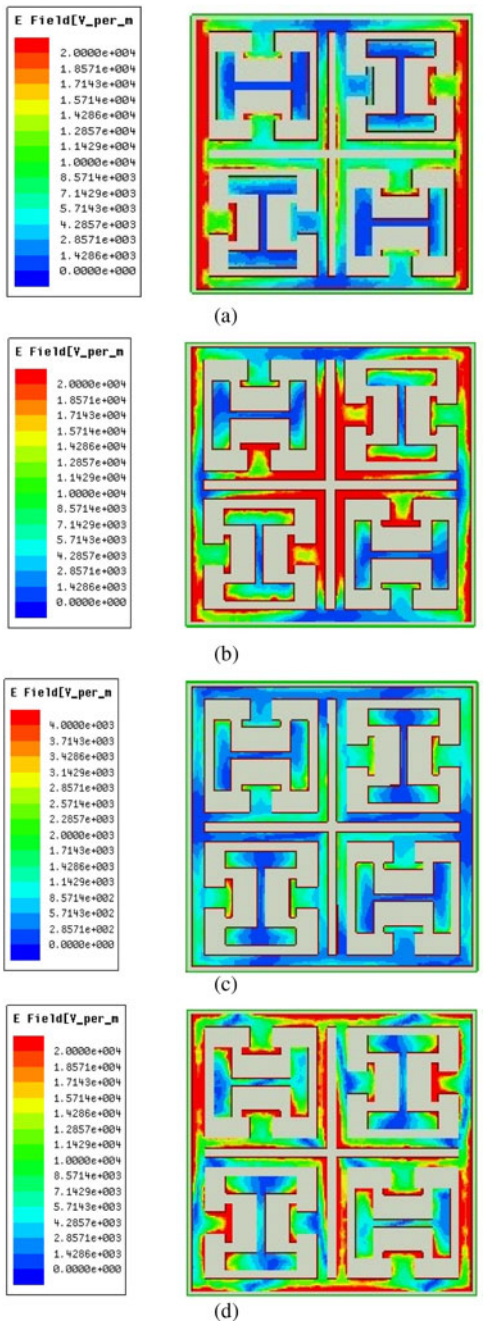

Fig. 9. Electric field distribution plot for the designed absorber structure at all the absorption frequencies. (a) At 3.40 GHz, (b) at 8.23 GHz, (c) at 9.89 GHz, (d) at 11.80 GHz.

(522.9 + 40.53j) is far away from free space impedance value, so absorption peak of 97.02% has occurred. However, at 8.23 and 9.89 GHz, the value of input impedance is (235 + 31.41j) and (209.8 + 17.85j, respectively. The value of input impedance is calculated using Equation (4) [28],

$$Z(\omega) = \eta_0 \sqrt{\frac{(1+S_{11})^2 - S_{21}^2}{(1-S_{11})^2 - S_{21}^2}} = \eta_0 \frac{1+S_{11}}{1-S_{11}}, \tag{4}$$

where $Z(\omega)$,η_0, represents input impedance, free space impedance, respectively.

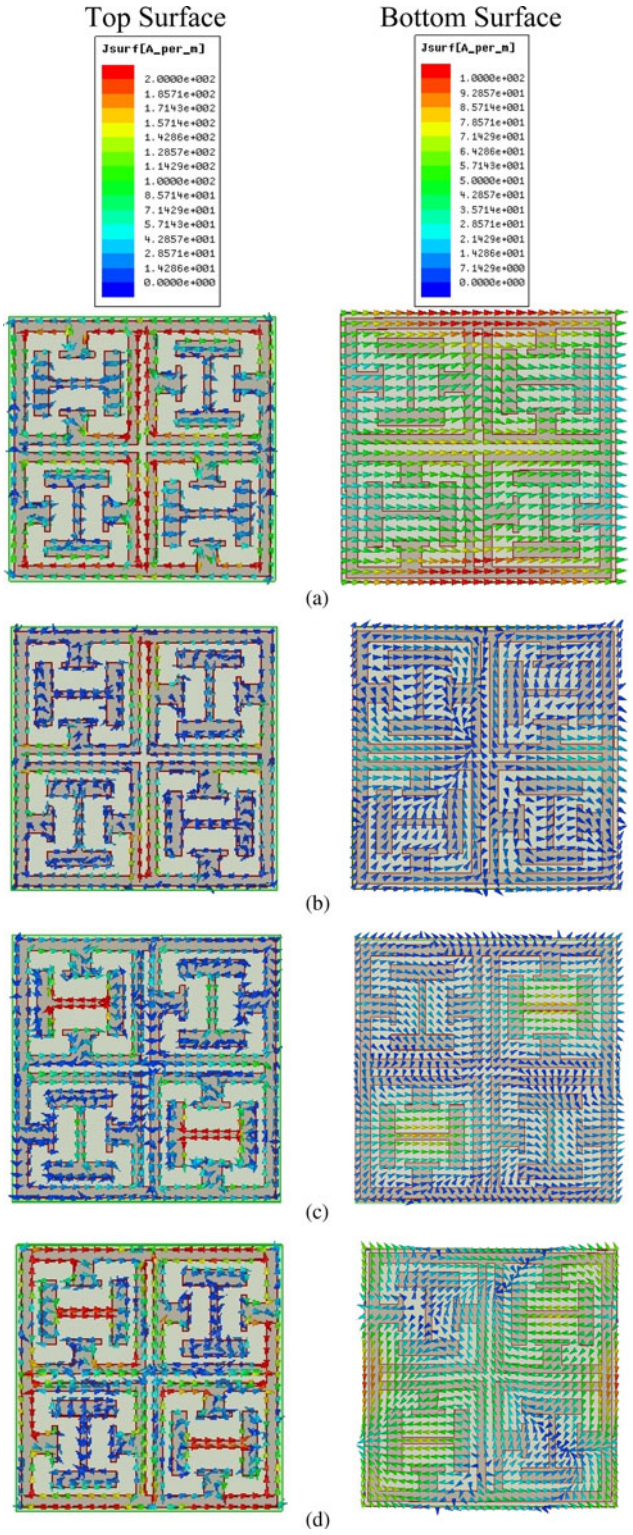

Fig. 10. Current density plot on top and bottom surfaces for the designed absorber structure at all the absorption frequencies.

Experimental results

In order to perform the experimental measurement, the prototype of designed absorber structure has been fabricated in a planar sheet of two-sided copper coated FR-4 epoxy dielectric substrate having dimensions of 12 mm × 12 mm × 1 mm. The

https://doi.org/10.1017/S1759078718000491 Published online by Cambridge University Press

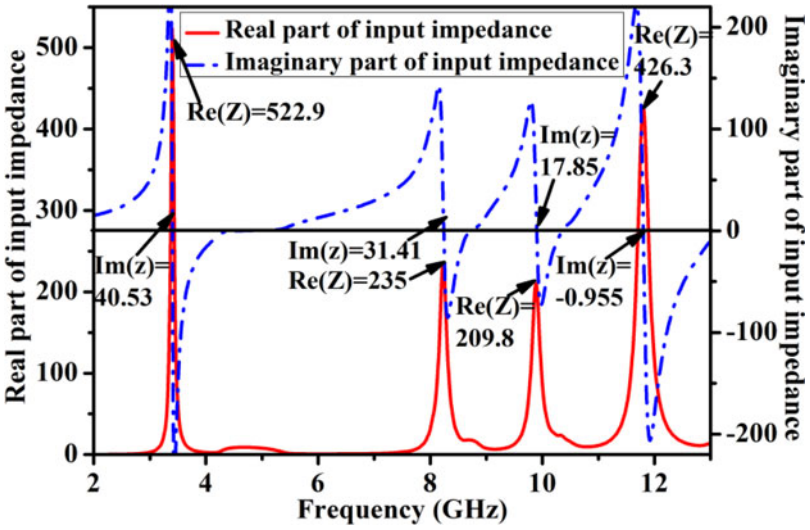

Fig. 11. Input impedance plot for the designed absorber structure.

fabricated proto-type along with a zoomed view of designed absorber has been shown in Fig. 12. A pair of horn antenna connected with Agilent N5221A PNA vectored network analyzer has been required to perform experimental measurement of fabricated proto-type. One horn antenna is used for transmission of EM wave while the other horn antenna is used for reception purpose. The entire experimental measurement has been done in free space.

Initially, the input reflection coefficient for the copper sheet (as a reference) has been measured. After that, the input reflection coefficient for the fabricated proto-type has been determined. The subtraction of the input reflection coefficient of the designed absorber proto-type with that of a reference copper sheet provides the actual value of the input reflection coefficients. Further, the absorptivity has been calculated from this actual value of the input reflection coefficient. Simulated input reflection coefficient plot along with the measured actual input reflection plot has been depicted in Fig. 13(a). Experimentally obtained peak absorption values for the designed absorber proto-type, shown in Fig. 13 (b), are 97% at 3.39 GHz, 93.98% at 8.21 GHz, 91.21% at 9.87 GHz, and 98.17% at 11.79 GHz. Further, the designed absorber proto-type offers experimental FWHM bandwidth of 240, 330, 340, and 460 MHz with respect to absorption peaks of 3.39, 8.21, 9.87, and 11.79 GHz. It has been seen that the simulated and measured absorption results are perfectly matched with each other. A slight deviation in absorption bandwidth, absorption peak, and presence of noise out of the absorption band may be occurred due to the free space measurement.

Table 1 shows the comparison of the performance of the proposed quad-band ultrathin absorber with the previously published articles.

Conclusion

In this paper, a compact metamaterial inspired ultra-thin polarization independent quad-band microwave absorber for EMI/EMC applications has been presented. Both the structures, structure-II, and structure-III, are responsible for the occurrence of four absorption peaks at the desired frequency. Metamaterial nature of the designed unit cell has been discussed through

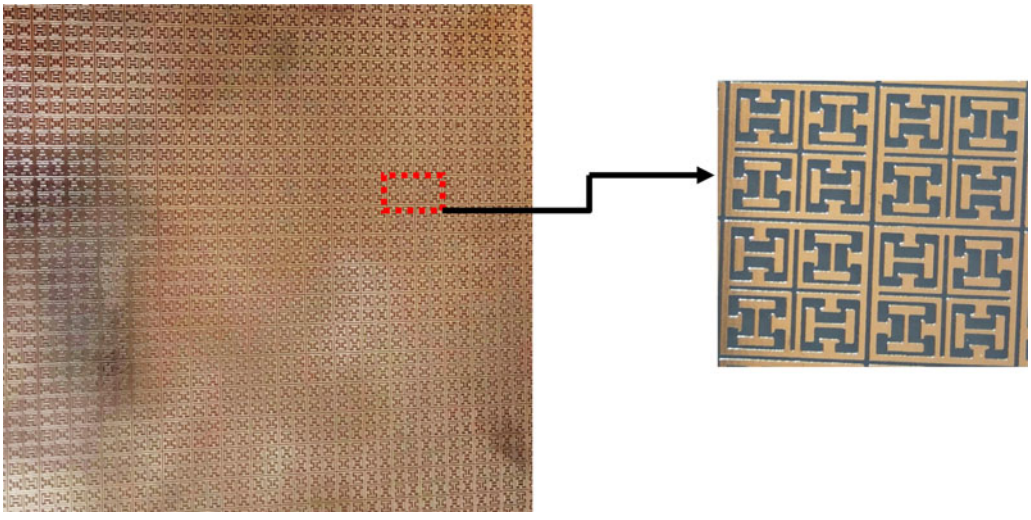

Fig. 12. Photograph of fabricated prototype along with its zoomed view.

https://doi.org/10.1017/S1759078718000491 Published online by Cambridge University Press

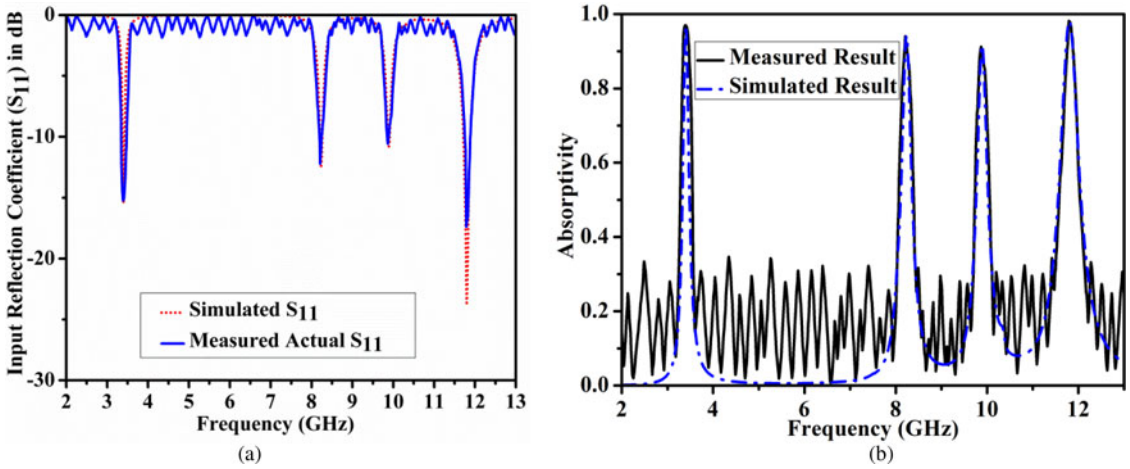

Fig. 13. (a) Measured and Simulated input reflection coefficient plot. (b) Measured and simulated absorption curves.

Table 1. Comparison of this work with previously published articles

Parameters	Absorption peaks (GHz)	Unit Cell Size (mm^3)	Unit cell size corresponds to lowest absorption peak (λ_0)	Number of bands	FWHM bandwidth corresponds to each absorption band (MHz)
This work	3.40, 8.23, 9.89, 11.80	12 × 12 × 1	0.136 × 0.136 × 0.011	Four	160, 280, 300, 520
[17]	8.65	7 × 7 × 0.7	0.201 × 0.201 × 0.020	One	331.8
[19]	2.45, 5.6	10 × 10 × 1	0.082 × 0.082 × 0.008	Two	–, –
[20]	3.07, 5.65, 8.11	18 × 18 × 1.5	0.184 × 0.184 × 0.015	Three	–, –, –
[21]	4.19, 9.34, 11.48	8 × 8 × 0.8	0.11 × 0.11 × 0.011	Three	170, 350, 480
[22]	3.25, 9.45, 10.90	11 × 11 × 1	0.12 × 0.12 × 0.011	Three	–, –, –
[23]	6.69, 7.48, 8.67, 9.91	20 × 20 × 1.14	0.446 × 0.446 × 0.025	Four	460, 510, 520, 440
[24]	4.34, 6.68, 8.58, 10.64	20 × 20 × 0.8	0.289 × 0.289 × 0.012	Four	170, 270, 400, 310
[25]	4.11, 7.91, 10.13, 11.51	15 × 15 × 1	0.206 × 0.206 × 0.014	Four	–, –, –, –

dispersion diagram plot. The proposed absorber exhibits compactness of $0.136\,\lambda_0 \times 0.136\,\lambda_0$ and ultra-thin thickness of $0.0113\,\lambda_0$ at lower absorption frequency of 3.40 GHz. Electric field distribution, current density, and input impedance plot have been studied to explain the absorption behavior of the designed metamaterial absorber. Due to the compact size, polarization independent characteristics, ultra-thin thickness, and quad-band metamaterial absorption, the proposed absorber structure can be used for several EMI/EMC applications.

Acknowledgement. This research work is supported by Science and Engineering Research Board (SERB), Department of Science & Technology (DST), Government of India, India under Project No. EMR/2016/002559.

References

1. **Caloz C and Itoh T** (2006) *Electromagnetic Metamaterials: Transmission Line Theory and Microwave Applications*. Hoboken, NJ: John Wiley & Sons, Inc.
2. **Shelby RA, Smith DR and Schultz S** (2001) Experimental verification of a negative index of refraction. *Science* **292**, 77–79.
3. **Veselago VG** (1968) The electrodynamics of substances with simultaneously negative values of ε and μ. *Soviet Physics Uspekh* **10**, 509–514.
4. **Mishra N and Chaudhary RK** (2016) A miniaturized ZOR antenna with enhanced bandwidth for WiMAX applications. *Microwave and Optical Technology Letters* **58**, 71–75.
5. **Mishra N, Gupta A and Chaudhary RK** (2015) A compact CPW-FED wideband metamaterial antenna using Ω-shaped interdigital capacitor for mobile application. *Microwave and Optical Technology Letters* **57**, 2558–2562.
6. **Fouad MA and Abdalla MA** (2014) New π-T generalised metamaterial negative refractive index transmission line for a compact coplanar waveguide triple band pass filter applications. *IET Microwaves, Antennas & Propagation* **8**, 1097–1104.
7. **Bilotti F, Tricarico S and Vegni L** (2010) Plasmonic metamaterial cloaking at optical frequencies. *IEEE Transactions on Nanotechnology* **9**, 55–61.
8. **Fang N, *et al.*** (2005) Sub – diffraction – limited optical imaging with a silver super lens. *Science* **308**, 534–537.
9. **Bilotti F, Nucci L and Vegni L** (2006) An SRR based microwave absorber. *Microwave and Optical Technology Letters* **48**, 2171–2175.
10. **Li H, *et al.*** (2011) Ultrathin multiband gigahertz metamaterial absorbers. *Journal of Applied Physics* **110**, 014909.
11. **Ghosh S, Bhattacharyya S and Srivastava KV** (2014) Bandwidth – enhancement of an ultrathin polarization insensitive metamaterial absorber. *Microwave and Optical Technology Letters* **56**, 350–355.
12. **Landy NI, *et al.*** (2008) Perfect metamaterial absorber. *Physical Review Letters* **100**, 207402.

https://doi.org/10.1017/S1759078718000491 Published online by Cambridge University Press

13. **Dimitriadis A, Kantartzis N and Tsiboukis T** (2012) A Polarization – angle – insensitive, bandwidth – optimized, metamaterial absorber in the microwave regime. *Applied Physics A* **109**, 1065–1070.
14. **Grant J, *et al.*** (2011) Polarization insensitive, broadband terahertz metamaterial absorber. *Optics Letters* **36**, 3476–3478.
15. **Avitzour Y, Urzhumov YA and Shvets G** (2009) Wide – angle infrared absorber based on a negative – index plasmonic metamaterial. *Physical Review B* **79**, 045131.
16. **Meng L, *et al.*** (2013) Polarization – sensitive perfect absorbers at near – infrared wavelengths. *Optics Express* **21**, A111–A122.
17. **Thummaluru SR, Mishra N and Chaudhary RK** (2016) Design and analysis of an ultra-thin X-band polarization – insensitive metamaterial absorber. *Microwave and Optical Technology Letters* **58**, 2481–2485.
18. **Zhai H, *et al.*** (2013) A dual-band wide-angle polarization-insensitive ultrathin gigahertz metamaterial absorber. *Microwave and Optical Technology Letters* **55**, 1606–1609.
19. **Bagci F and Medina F** (2017) Design of a wide-angle, polarization-insensitive, dual-band metamaterial-inspired absorber with the aid of equivalent circuit model. *Journal of Computational Electronics* **16**, 913–921.
20. **Bian B, *et al.*** (2013) Novel triple-band polarization-insensitive wide-angle ultra-thin microwave metamaterial absorber. *Journal of Applied Physics* **114**, 194511.
21. **Mishra N, *et al.*** (2017) An investigation on compact ultra-thin triple band polarization independent metamaterial absorber for microwave frequency applications. *IEEE Access* **5**, 4370–4376.
22. **Zhai H, *et al.*** (2015) A triple-band ultrathin metamaterial absorber with wide angle and polarization stability. *IEEE Antennas and Wireless Propagation Letters* **14**, 241–244.
23. **Zheng D, *et al.*** (2013) Four-band polarization-insensitive metamaterial absorber based on flower-shaped structures. *Progress In Electromagnetic Research* **142**, 221–229.
24. **Agarwal M, Behera AK and Meshram MK** (2016) Wide-angle quad-band polarisation-insensitive metamaterial absorber. *Electronics Letters* **52**(5), 340–342.
25. **Chaurasiya D, *et al.*** (2016) Compact multi-band polarisation-insensitive metamaterial absorber. *IET Microwaves, Antennas & Propagation* **10**(1), 94–101.
26. **Huang L and Chen H** (2011) Multi-band and polarization insensitive metamaterial absorber. *Progress In Electromagnetics Research* **113**, 103–110.
27. **Mehdipour A, Denidni TA and Sebak AR** (2014) Multi-band miniaturized antenna loaded by ZOR and CSRR metamaterial structureswith monopolar radiation pattern. *IEEE Transactions on Antennas and Propagation* **62**, 555–562.
28. **Smith DR, *et al.*** (2005) Electromagnetic parameter retrieval from inhomogeneous metamaterials. *Physical Review E* **71**, 036617.

Naveen Mishra was born in Deoria (Uttar Pradesh), India on October 04, 1990. He received the B. Tech. degree in electronics and communication engineering from Uttar Pradesh Technical University, Lucknow in 2010. Currently, he is pursuing Ph.D. from Department of Electronics Engineering, Indian Institute of Technology (Indian School of Mines), Dhanbad, India. He joined the Department of Electronics Engineering, Indian Institute of Technology (Indian School of Mines), Dhanbad, in January 2014, as a Junior Research Fellow, where he has been a Senior Research Fellow since January 2016. He has authored or co-authored more than 24 research articles in international/ national journals/ conference proceedings. His current research interests involve Metamaterials structures and its applications.

Khusboo Kumari was born in Koderma (Jharkhand), India on February 13, 1992. Currently, she is pursuing M. Tech. from Department of Electronics Engineering, Indian Institute of Technology (Indian School of Mines), Dhanbad. She did her B. Tech. from Vinoba Bhave University, Hazaribag in 2013. Her current research topic is Design and Development of Ultra-thin Metamaterial Absorber.

Dr. Raghvendra Kumar Chaudhary is working as an Assistant Professor at Department of Electronics Engineering, Indian Institute of Technology (Indian School of Mines), Dhanbad, India. He did his Ph.D. from Indian Institute of Technology Kanpur, India in January 2014, the M.Tech. degree from Indian Institute of Technology (BHU), Varanasi, India, in 2009, and the B.Tech. degree from University Institute of Engineering and Technology, Kanpur India, in 2007. Dr. Chaudhary has authored more than 125 referred Journal and Conference papers. He was the recipient of the International Travel Grant form CSIR, DST, and IIT Kanpur, India. He was the recipient of the Best Student Paper Bronze Award at IEEE APACE, Malaysia in 2010 and also the recipient of the Best Paper Award at ATMS, India in 2012. He is a member of IEEE and potential reviewer of many journals and conferences such as IEEE Transactions on Antennas & Propagation, IEEE AWPL, IET MAP, IET Electronics Letters etc. His current research interests involve Metamaterials, Dielectric Resonators, and Computational Electromagnetics. He is presently handling many research projects in the capacity of Principal Investigator sponsored by Indian funding agencies like SERB(DST), ISRO etc.

https://doi.org/10.1017/S1759078718000491 Published online by Cambridge University Press